

Chapter I.7

Concepts for Integration of Measurements and Methods

Domenico Cimini

1 Introduction

Ground-based remote sensing observations of atmospheric variables are collected in many sites worldwide for several applications, ranging from weather monitoring, meteorology, climatology, aviation support, etc.

Since radiation interacts with the atmosphere depending upon its wavelength, spectrally diverse measurements contain different information about the atmospheric state and composition. Each instrument is sensitive to a limited number of atmospheric variables and thus provides information about one or a few aspects of the atmosphere, with the associated uncertainty and limitations. When observations from different instruments are available at the same site and time, a broader view of the atmospheric process can be achieved. Thus, typically an atmospheric observatory operates several different instruments in a single location, simultaneously and continuously. Some instruments use technology that is mature and well understood, while other instruments have been recently developed as research units. A major focus of current remote sensing research is to evaluate the capability of the existing instruments to remotely derive meteorological quantities using sensor synergy. A synergetic approach, relying on the complementary characteristics of different instrumentations, is sometimes able to either improve retrieval accuracy, overcome limitations, or provide additional products with respect to what is possible with single instruments. This contribution reviews the motivations, presents few examples, and discusses present challenges of ground-based remote sensing instrument integration.

D. Cimini (✉)
IMAA/CNR, C.da S. Loja, Tito Scalo (PZ), Italy
e-mail: cimini@imaa.cnr.it

2 Motivations and Challenges

In the last four decades, large efforts have been undertaken to develop ground-based instruments for continuously monitoring the atmosphere. Ground-based remote sensing instruments based on different physical principles and working at different wavelengths of the electromagnetic (EM) spectrum are diversely sensitive to the different atmospheric properties. Thus, instrumentations are able to observe diverse aspects of the atmosphere, such as composition, motion, and thermodynamical properties (temperature, humidity, etc.).

For example, as described in the previous chapters and summarized in Table I.7.1, microwave and infrared radiometers are sensitive to atmospheric temperature, humidity, cloud content, and microphysics; elastic, Raman, and Doppler lidars are sensitive to atmospheric aerosols, temperature, and wind; weather and cloud radars are sensitive to precipitating and non-precipitating hydrometeors; wind profiler radars and sodars are sensitive to wind direction and speed. Each of these atmospheric parameters can be retrieved from ground-based observations with some

Table I.7.1 A list of atmospheric variables and the associated instrumentation which is able to provide useful information (extended from Ackerman and Stokes, 2003)

Atmospheric variables	Instrument type
Surface radiation budget	Broad band solar and IR radiometers Shadow-band radiometer (narrow spectral bands) Spectrometer (400–3,000 nm) Infrared interferometer (3–20 μm)
Atmospheric temperature profile	Microwave radiometer Infrared interferometer (3–20 μm) Raman lidar
Water vapor profile	Microwave radiometer (24–31 GHz) Infrared interferometer (3–20 μm) Raman lidar
Aerosol profile	Elastic lidar
Particle optical depth	Narrow-band sun photometer Shadow-band radiometer
Cloud presence and location	Ceilometer Lidar Millimeter-wave radar
Cloud properties	Lidar Millimeter-wave radar Radiometers (solar, IR, microwave)
Wind profile	Wind profiler radar Sodar Elastic lidar
Composition (trace gases)	Multichannel narrow-band radiometer Infrared interferometer
Precipitation	Weather radar Microwave radiometer Disdrometer

degree of accuracy and certain advantages and limitations. However, instead of a single instrument, quite commonly a variety of ground-based instrumentation is deployed at the same site in order to cover more than one aspect of the atmosphere at the same time. While these instruments are typically used in standalone mode, their combination offers new possibilities to overcome intrinsic limitations. For example, a single instrument/technique may present limitations related to short range of application, poor spatial resolution, poor accuracy, ambiguous solution, simultaneous sensitivity to more than one parameter, or a combination of the above. In other words, each single instrument provides information about one or more parameters with the accuracy and the limitations associated with the used technology and technique, but sometimes part of these limitations may be overrun by the synergetic use of the other independent instrumentation operating at the same site. In addition, a new set of products may be generated combining complementary information from independent instruments. In a problem-solving framework, a synergetic approach would put further constraints to the solution of the atmospheric state's estimate.

Thus, since theoretical and technology research is dedicated to reducing the limitations and to increasing the performances of remote sensing, it is of uttermost importance to investigate the actual information content that can be gained from the optimal combination of existing instrumentation. For this purpose, a significant effort is dedicated to the establishment of atmospheric observatories equipped with state-of-the-art technology, the so-called anchor stations, where new methods are developed and tested for retrieving the most complete picture of the atmospheric profiles and their errors (Engelbart et al., 2009). One of the most important European atmospheric anchor observatories, the Cabauw Experimental Site for Atmospheric Research (CESAR) in the Netherlands, is pictured in Fig. 1.7.1.



Fig. 1.7.1 A picture of the CESAR observatory in Cabauw, the Netherlands. CESAR is one of the European anchor station for atmospheric in situ and atmospheric remote sensing (picture courtesy of Herman Russchenberg, Delft University of Technology)

The concept of an integrated approach relies on finding observations that can be used in synergy for either estimating a parameter with better accuracy or getting information about new parameters that can be derived from the ones obtained by the single instruments. Therefore, the characteristics of the instrumentation taking part in an integrated approach should be

- providing independent observations (different instruments)
- providing complementary observations (different spectral regions, viewing angles, active/passive methods)
- measuring different aspects of the atmosphere
- sensing a somewhat common observation volume

However, integrating measurements and methods involves more than one challenge. First of all, an integrated approach requires the development of a multi-input algorithm producing results that are physically consistent with all the observations. This in turn requires a well-understood theory or alternatively the a priori knowledge of a statistically significant data set. Moreover, with regard to the operational implementation there is always a concern for implementing and maintaining algorithms taking input data from independent instrumentation, since it is well known that more data streams bring inevitably more troubles. Finally, it must be demonstrated that the benefits coming from the integrated approach are significant to justify the extra effort and costs involved in the development and maintenance of instruments and methods.

3 Examples from the Field

Several examples of integrated approaches using different ground-based instruments and observations can be found in the open literature from the last decade (Han et al., 1997; Stankov et al., 1996; Mace et al., 2001; Löhnert et al., 2004). In those and other papers both physical and statistical methods are used to retrieve atmospheric parameters from ground-based observations. In case the physical process of the radiation–atmosphere interaction is properly understood, retrieval algorithms can be made physically consistent. This approach is used when the theory is well understood and the relationships between the variables and the observations are analytically solvable and easy to invert and implement. Conversely, if the relationships between the variables and the observations are not analytically solvable and/or difficult to invert and implement, statistical methods are typically used. Thus, this approach is often used when the retrieved parameter is linked to the observations by complex relationships with a large number of degrees of freedom.

In the following, few examples of successful sensor synergy are briefly described; the interested reader may refer to the original papers for further details. Of course, this list does not mean to be complete and many other techniques are available in the open literature.

3.1 Synergy of Active and Passive Observations for Increasing Water Vapor Vertical Resolution

Monitoring of humidity profiles in the lower troposphere has been one of the main goals of recent meteorological research due to its importance for atmospheric dynamics and microphysics. An appealing application to the retrieval of whole-weather high-resolution atmospheric humidity profiles is the synergetic use of ground-based instruments only, such as either a combination of radar wind profilers and global position system (GPS) receivers or either a combination of radar wind profilers and microwave radiometers (Stankov et al., 1996; Gossard et al., 1999; Furumoto et al. 2003; Bianco et al., 2005). In particular, the last approach has significant potential due to the profiling capability of both sensors and the possibility to estimate the atmospheric state in terms of wind, humidity, and temperature. Thus, algorithms to compute atmospheric humidity high-resolution profiles by synergetic use of microwave radiometer profiler (MWRP) and wind profiler radar (WPR) were developed in the last decade. The technique described in Bianco et al. (2005) is based on the processing of WPR data for estimating the potential refractivity gradient profiles and on the combination with MWRP estimates of potential temperature profiles in order to fully retrieve humidity gradient profiles. To retrieve high-resolution humidity profiles in this combined approach, the zeroth, first, and second moments, computed by a fuzzy logic algorithm, are employed to compute the structure parameter of potential refractivity (C_ϕ^2), the horizontal wind (V_h), and the structure parameter of vertical velocity (C_w^2). The quantities C_ϕ^2 , V_h , and C_w^2 can then be properly used together to retrieve the potential refractivity gradient profiles ($d\phi/dz$). On the other hand, microwave radiometer data can be used to estimate the potential temperature gradient profiles ($d\theta/dz$). As a final step of the combined retrieval technique, profiles of $d\phi/dz$, derived from WPR, and of $d\theta/dz$, derived from MWRP, are sufficient to fully estimate humidity gradient profiles. The advantage of such a synergetic humidity retrieval technique is to increase the vertical resolution of MWRP, without losing the high accuracy it can provide for integrated values, and to be completely independent from simultaneous radiosonde observations.

The basic principles of the theory used for the retrieval of vertical humidity profiles with the combined use of $d\phi/dz$ from WPR and $d\theta/dz$ from MWRP are summarized below. Radar-obtained values of $d\phi/dz$ are derived combining V_h , C_ϕ^2 , and C_w^2 , which are respectively related to the first, zeroth, and second moments calculation of the radar-derived spectra acquisitions (Stankov et al., 2003). Gossard et al. (1982, 1998) found that for homogeneous isotropic turbulence in a horizontally homogeneous medium with vertical gradients of mean properties, the vertical gradient of potential refractivity is

$$\left(\frac{d\phi}{dz}\right)^2 \approx \left(\frac{L_w}{L_\phi}\right)^{4/3} \left(\frac{dV_h}{dz}\right)^2 \left(\frac{C_\phi}{C_w}\right)^2, \quad (1)$$

where L_w and L_ϕ are the outer length scales for potential refractive index and shear defined in Gossard et al. (1982).

Considering the given definition of the potential temperature θ , we can estimate this quantity and its vertical gradient by using the temperature profile as retrieved by the MWRP together with the measurements of surface pressure and a prediction of the atmospheric scale height:

$$\frac{dQ}{dz} = (b_0)^{-1} \left[\frac{d\phi}{dz} + a_0 \frac{d\theta}{dz} \right], \quad (2)$$

which gives the vertical profile of humidity gradient as a function of vertical profiles of potential refractivity and potential temperature gradients. By integrating the vertical profile of dQ/dz we can, therefore, compute the vertical profile of Q .

Figure I.7.2 presents results relative to a case study (Bianco et al. 2005). Note that the humidity profile is scaled in order to match the MWRP water vapor content, integrated up to the maximum height reached by the WPR measurement. This is an

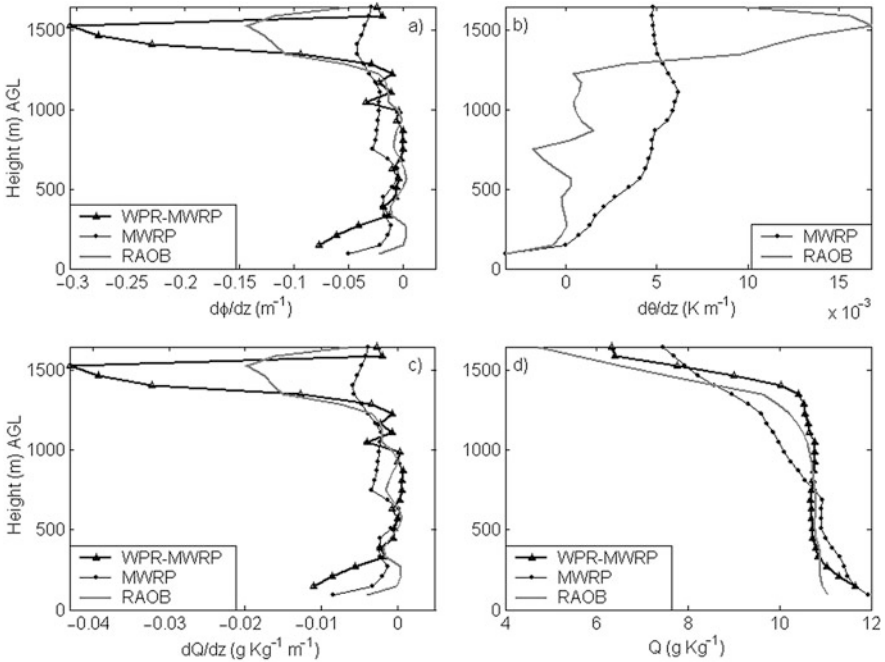


Fig. I.7.2 a) Hourly vertical profiles for $d\phi/dz$ as measured by radiosonde (solid grey line), estimated by MWRP (dotted line), and computed with the combined technique (solid black line with triangles); b) $d\theta/dz$ as measured by radiosonde (solid grey line) and estimated by MWRP (dotted line); c) hourly vertical profiles for dQ/dz as measured by radiosonde (solid grey line), estimated by MWRP (dotted line), and computed with the combined technique (solid black line with triangles at measurement heights); d) retrieved humidity vertical profiles (Q) obtained from the integration of dQ/dz (after Bianco et al., 2005)

important step because it guarantees that the original MWRP accuracy for integrated water vapor content is preserved in the product of the combined technique.

3.2 *Integrated Approach for the Retrieval of Physically Consistent Profiles*

Continuous and accurate profiles of temperature, humidity, and hydrometeor content at high temporal and spatial resolution are extremely important for evaluating and improving model forecasts, parameterization schemes, and satellite retrieval algorithms.

Integrated methods for deriving physically consistent profiles of temperature, humidity, and cloud liquid water content were developed in the last years (Han et al., 1997; Stankov et al., 1996; Löhnert et al., 2004). The method described in Löhnert et al. (2004) combines a ground-based multichannel microwave radiometer (MWR), a cloud radar, a lidar ceilometer, the nearest operational radiosonde measurement, and ground-level measurements of standard meteorological properties with statistics derived from the results of a microphysical cloud model. The described method, called the integrated profiling technique (IPT), is general and can be extended to include other instruments and observations. All measurements are integrated within the framework of optimal estimation to guarantee a retrieved profile with maximum information content. The IPT uses the so-called optimal estimation equations directly derived from Bayes's theorem considering a linear forward model and Gaussian-distributed variables. Given the set of measurements, the optimal estimation inversion procedure finds a solution that satisfies the measurements after the forward model has been applied to the retrieved parameters. In the context of IPT, the microwave radiative transfer equation and a relationship between the radar reflectivity Z and the liquid water content (LWC) profiles are regarded as the valid forward model.

A prerequisite of the IPT is an accurate knowledge of the error characteristics of each measurement and of the forward model by means of covariance matrices. Measurements with small errors will have a higher weight in the solution than measurements with large errors; the same applies for the accuracy level of the description of the relationship between the observations and the atmospheric parameters.

The forward model F performs the radiative transfer calculation [Eq. (30) in Chap. I.1] where \mathbf{K} is the Jacobi matrix, and $\mathbf{K} = dF/d\mathbf{x}$. The parameter vector \mathbf{x} consists of the profiles of T , q , and LWC. The measurement vector \mathbf{y} consists of the MWR brightness temperatures (T_b), the radar reflectivity profile at detected cloud levels, and the ground-level measurements of temperature and humidity. Following Rodgers (2000), the optimal estimation equation for this problem is written as

$$\mathbf{x}_{i+1} = \mathbf{x}_i + \left(\mathbf{B}^{-1} + \mathbf{K}_i^T \mathbf{R}^{-1} \mathbf{K}_i \right)^{-1} \left[\mathbf{K}_i^T \mathbf{R}^{-1} (\mathbf{y} - F(\mathbf{x}_i)) - \mathbf{B}^{-1} (\mathbf{x}_i - \mathbf{x}_b) \right], \quad (3)$$

where i represents the iteration step, \mathbf{R} the combined measurement and forward model error covariance matrix, and \mathbf{B} the a priori covariance matrix.

Atmospheric temperature and humidity are assumed as Gaussian-distributed parameters, while for LWC the value of $10 \log_{10}(\text{LWC})$ is retrieved, which more closely resembles a Gaussian-distributed parameter than LWC itself. Other assumptions are that the random errors prevail in the T_b and the errors of Z in the units of dBZ are also Gaussian distributed.

Equation (3) is iterated i_{op} times in i (\mathbf{K}_i is recalculated after each iteration step) until a minimum of a cost function is found, yielding the solution \mathbf{x}_{op} . Following Rodgers (2000), the iteration stops upon reaching convergence by considering a quadratic cost function between $F(\mathbf{x}_i)$ and $F(\mathbf{x}_{i+1})$:

$$[F(\mathbf{x}_{i+1}) - F(\mathbf{x}_i)]^T \mathbf{S}^{-1} [F(\mathbf{x}_{i+1}) - F(\mathbf{x}_i)] \ll n(\text{obs}), \tag{4}$$

where \mathbf{S} is the covariance matrix between the measurement and $F(\mathbf{x}_{\text{op}})$ and $n(\text{obs})$ indicate the number of observations (i.e., the dimension of \mathbf{y}). The solution \mathbf{x}_{op} must be interpreted as the most probable solution of a Gaussian-distributed probability density function, whose covariance can be written as

$$\mathbf{S}_{\text{op}} = \left(\mathbf{K}_{i_{\text{op}}}^T \mathbf{R}^{-1} \mathbf{K}_{i_{\text{op}}} + \mathbf{B}^{-1} \right)^{-1}. \tag{5}$$

The diagonal elements of this matrix give an estimate of the mean quadratic error of \mathbf{x}_{op} . The physical consistency of the retrieval products is ensured by the fact that the retrieved profile will reproduce the measured radiation within the measurement accuracy.

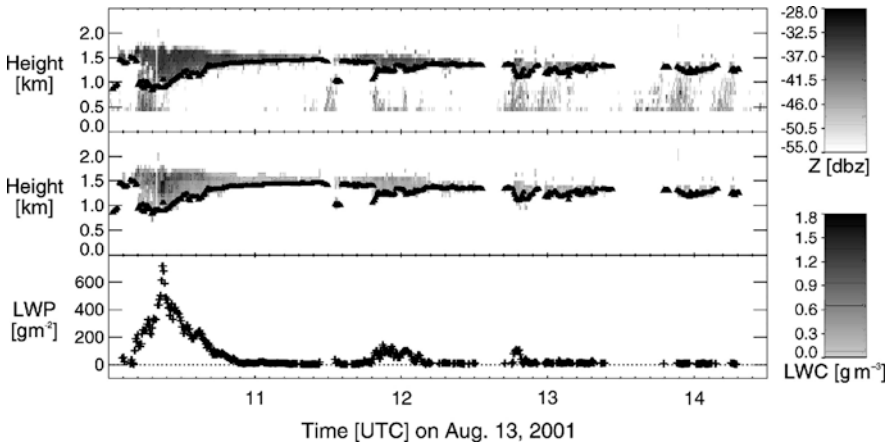


Fig. 1.7.3 Time series of (top) radar reflectivity, (center) IPT-LWC on radar resolution, and (bottom) vertically integrated LWC (LWP) at Cabauw, the Netherlands. The black triangles in the upper two panels indicate the lidar ceilometer cloud base (after Löhnert et al., 2004)

The developed IPT was applied to both synthetic and experimental data. It was shown that the profiles obtained with the IPT are significantly more accurate than those obtained with other more common methods. Error analysis indicates root-mean-square (rms) uncertainties of less than 1 K in temperature and less than 1 g/m³ in humidity, where the relative error in liquid water content ranges from 15 to 25% (considering liquid phase non-precipitating clouds only). Figure 1.7.3 presents time series of radar reflectivity and LWC retrievals over CESAR.

The formulation of IPT allows the incorporation of multiple measurements into the retrieval. Thus, the IPT represents a major step toward the synergy of arbitrary measurements and their integration to form a product that increasingly resembles reality. The natural evolution is the development of an “all encompassing” algorithm that can take into account all instruments operating momentarily at a specific station and deliver the best estimates of profiles of temperature, humidity, and cloud hydrometeors during all weather conditions.

3.3 Combination of Active and Passive Measurements for the Investigation of Cirrus Clouds

Cirrus clouds play an important role in increasing the greenhouse capacity of Earth’s climate system. In fact, these high cloud layers are composed of ice crystals and typically reflect less solar radiation than do water clouds, but absorb significant amounts of thermal infrared radiation emitted by the ground and the lower atmosphere. In spite their importance, cirrus clouds are notoriously difficult to model, because the processes that create them are complex and not completely understood. Direct observation from aircraft is problematic because their altitude and laboratory experiments cannot adequately capture the complexity of cirrus cloud formation in the free atmosphere. Conversely, ground-based remotely sensing techniques offer the opportunity to greatly increase the understanding of cirrus clouds microphysics (Ackerman and Stokes, 2003).

As an example, techniques combining millimeter-wave cloud radar (MMCR) observations with thermal infrared interferometry have been developed by the US Department of Energy’s Atmospheric Radiation Measurement (ARM) program for the study of cirrus clouds; results are used to compile cirrus cloud statistical distribution and empirical relationships for the parameterization to be used in climate models (Mace et al., 2001).

The method takes advantage of the different instrumental sensitivities to determine the integrated column ice mass and the mean ice particle size. The radar directly measures the height and extent of cirrus clouds, and the magnitude of the backscattered radar signal depends on the total ice mass and the distribution of particle sizes. The downward radiance measured by the infrared interferometer is a combination of thermal emission by atmospheric water vapor and by the cloud ice mass. From the radar and the infrared data, together with balloon measurements of atmospheric temperature and moisture, the developed method deduces the emission from the clouds alone (Mace et al., 1998).

The radar measures the backscatter cross section per unit volume and this cross section can be expressed in terms of the radar reflectivity factor

$$Z = \int_0^{\infty} N(D) \cdot D^6 \cdot dD. \quad (6)$$

Assuming that the layer-mean particle distribution can be adequately described by a modified gamma function in terms of the modal diameter D_x , the number of particles per unit volume per unit length N_x , and the order of the distribution α :

$$N(D) = N_x \exp(\alpha) \left(\frac{D}{D_x} \right) \exp \left[-\frac{D\alpha}{D_x} \right], \quad (7)$$

then the variables of interest, namely the integrated column ice mass and the mean ice particle size, can be derived as

$$\text{IWP} = \rho_i \frac{\pi}{6} \bar{Z} \frac{\alpha^3 (3 + \alpha)!}{D_x^3 (6 + \alpha)!} \Delta h \quad (8)$$

$$r_e = \frac{D_x (3 + \alpha)!}{2(2 + \alpha)!} \alpha^\alpha. \quad (9)$$

The two unknown parameters of the modified gamma distribution can be determined from the observed downwelling radiance and the radar reflectivity using an expression of the cloud layer emittance. Using the observed radar reflectivity and the layer emittance determined from the downwelling radiance the problem is solved numerically. The ice water path and particle size are finally calculated using Eqs. (8) and (9).

3.4 Observations Synergy for Improving the Understanding of Radiative Transfer

Longwave and solar radiative transfer are the prime physical mechanisms that drive the circulation and temperature structure of the atmosphere, and radiative processes play a central role in most climate change mechanisms.

Parameterization is required to account for the radiant energy transport in global climate models (GCM), as the full treatment of the radiative transfer is prohibitively computationally expensive. Detailed radiative transfer models that incorporate all of the known physics, such as line-by-line models, are typically used to construct significantly faster radiation models to calculate radiative fluxes in GCMs. The line-by-line model used to build these faster models must be accurate, as even 1% changes in radiation are significant for climate. In addition, improvements in the understanding of the spectral radiative transfer are important for computing

the atmospheric cooling rate profiles and for the enhancement of remote sensing applications.

In this perspective, a suite of independent ground-based observations is valuable for investigating the radiative properties of the atmosphere using radiation closure experiments. This kind of approach typically leads to reducing the uncertainties on a radiative-relevant parameter or to solve the ambiguity that may arise from observation taken with a reduced set of instruments.

Research funded by the ARM program has led to significant improvements in high spectral resolution radiative transfer modeling over the last decade. The ARM program supported a variety of projects, including laboratory spectroscopic studies and field experiments, such as the pilot radiation observation experiment (PROBE; Westwater et al. 1999).

At the ARM Cloud and Radiation Testbed sites, quality measurement experiments (QME) that compare observations and state-of-the-art calculations for the improvement of radiative transfer calculations have been ongoing since more than a decade. The QMEs have been used to

- (1) validate and improve the absorption models and spectral line parameters used in line-by-line radiative transfer models
- (2) assess the ability to define the atmospheric state used in the model calculation
- (3) assess the quality of the radiance observations that serve as ground truth for the model

QME can be used to investigate the absorption due to a variety of trace gases; in particular, Turner et al. (2004) focused on water vapor absorption because of the large impact this absorption has on the radiative flux calculations. Turner et al. (2004) used data from the ARM Southern Great Plains site in Oklahoma, hosting a wide variety of ground-based instrumentation designed to meet the goal of collecting a long-term data set that can be used to improve climate models. Of particular importance of this application are the atmospheric emitted radiance interferometer (AERI), radiosondes, microwave radiometer (MWR), Raman lidar, and micropulse lidar (MPL).

In Turner et al. (2004), the measures taken into the QME for reducing and accounting the uncertainties related to the instruments (calibration, accuracy) and the atmospheric state (water vapor content, cirrus cloud presence) are discussed. Improvements made to the various instruments and the data streams resulting from the original analysis allowed to generate a new QME that addressed most of the issues that limited the original data set. For example, new operational calibration routines were developed for the MWR, radiosonde humidity were scaled based on MWR IWV, and Raman lidar depolarization ratio was used to screen cases corrupted by thin cirrus.

A trustworthy data set of observations from all the above instruments has been carefully constructed and used to quantitatively evaluate a state-of-the-art line-by-line radiative transfer model (LBLRTM) in order to reduce its modeling uncertainties.

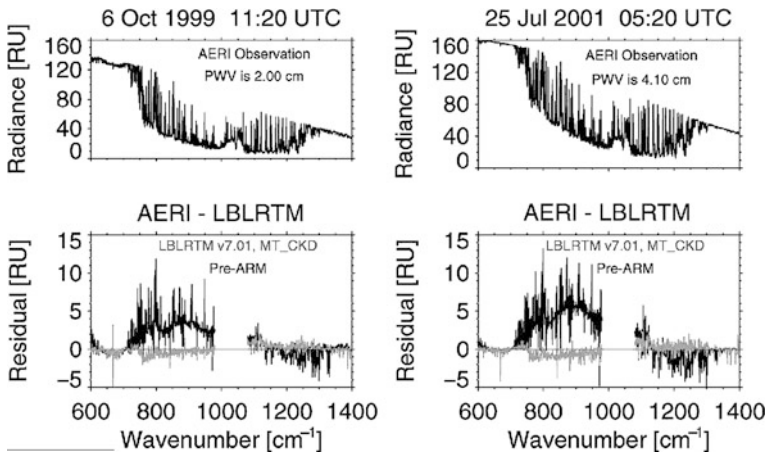


Fig. I.7.4 (*upper left*) Observed AERI spectra for a midlevel (2.0 cm) and (*upper right*) high (4.1 cm) IWV cases, along with (*lower left, lower right*) the observed minus calculated residuals for two different models. The residuals in *black* demonstrate the state of the art in the early 1990s. The residuals in *grey* indicate the improvements obtained by ARM scientists up to 2004 (after Turner et al., 2004)

Figure I.7.4 demonstrates the large improvement in the modeling of high spectral resolution downwelling radiation over the past decade. These improvements, which have generally come in small incremental changes, were made primarily in the water vapor self- and foreign-broadened continuum and the water vapor absorption line parameters. Note that the pre-ARM results had much larger errors in both the line parameters as well as the underlying continuum as compared to the current state of the art. These changes, when taken as a whole, result in up to a 6 W/m^2 improvement in the modeled clear-sky downwelling longwave radiative flux at the surface and significantly better agreement with spectral observations and downwelling longwave fluxes to be calculated with an accuracy of better than 2 W/m^2 .

3.5 Radar–Lidar synergy for the Detection of Cloud Boundaries and Target Classification

Frequent and detailed information about the extension of hydrometeor and aerosol layers in the atmosphere is crucial for weather forecast, climate model parameterization, and atmospheric science in general. Therefore, precise detection of fog and cloud boundaries is a major application for ground-based remote sensing sensors, and the combination of a cloud radar and a lidar ceilometer offers a powerful tool for the detection of these parameters. In fact, cloud radars can be used to gain insight into the vertical position and structure of the cloud. However, the radar reflectivity

Z is proportional to the sixth moment of the cloud drop size distribution. Conversely, for lidar ceilometers the backscattered radiation is proportional to the droplet diameter squared because of the wavelength being much shorter than the particle diameter (i.e., optical regime limit). Accordingly, lidar ceilometers are more sensitive to small cloud particles than cloud radars, which in turn are highly sensitive to larger drops. Thus, lidar ceilometer measurements are more accurate in deriving the actual cloud-base height while cloud radars often detect light drizzle below the actual cloud base. Conversely, lidar ceilometers are usually not able to detect the vertical cloud structure because most liquid water clouds are optically thick in the visible range such that the lidar ceilometer signal will almost always be extinguished in the lower part of the cloud. In the detection of cloud boundaries, cloud radar and lidar ceilometer have clearly complementary features.

A radar–lidar combined technique starts searching for one or more cloud layers into the lidar ceilometer backscattered signal, using the fact that to lidar the base of liquid clouds appears as a strong echo that is confined over only a few hundred meters. Liquid cloud base is defined as the lowest pixel for which the difference in the backscattered signal between it and the pixel above exceeds a certain threshold. Lidar cloud top is defined as the last non-zero pixel just below the level where the lidar signal falls to 0. Then the radar profile is analyzed to determine cloud top in the case that the lidar has been extinguished while the radar still has a signal. Thus the bases and tops of each of the liquid clouds in the profile are determined.

In addition, a proper combination of cloud radar and lidar ceilometer observations is able to provide information on the LWC within the cloud and a classification of the liquid cloud into three regimes: non-drizzling cloud, cloud-in-transition, and drizzling clouds (Krasnov and Russchenberg, 2002). Note that such an LWC retrieval works for liquid water clouds only and thus it requires a pre-screening of the atmospheric situation.

For these purposes, target categorization methods have been developed based on ground-based observations. For example, an integrated technique based on instrument synergy for target categorization has been developed within the Cloudnet project (www.cloud-net.org). In this technique, each pixel is categorized in terms of the presence of liquid droplets, ice, insects, aerosol, etc., thereby allowing algorithms specific to one type of target to be applied (Hogan and O'Connor, 2004).

4 Conclusions

In summary, the rationale behind the efforts to combine measurements and methods can be generalized as twofold:

- to derive additional parameters that are not otherwise derived and
- to maximize performances of retrieved parameters.

Therefore, the characteristics of the instrumentation taking part of an integrated suite should be

- independent observations
- complementary observations
- measuring different aspects of the atmosphere, and
- sensing a common observation volume

Note that the successful application of ground-based integrated systems depends upon their cost for deployment and maintenance; as a consequence, the preference should go to sensors and methods that are:

- cost-effective
- robust and easy to apply and maintain, and
- suitable for network deployment

Currently there are several research proposals and ongoing projects that focus on the establishment of a number of integrated observation sites with a selection of different remote and in situ observation instruments.

In summary, the ideal integrated remote sensing station for climate, meteorology, and civil protection applications would be comprised of a number of cost-effective, unattended, easy to maintain, robust, and stable instruments for providing the essential atmospheric variables. The observations would have good quality, with high spatial and temporal resolution and it would be possible to integrate the different measurements into ready-to-use products that meet the user requirements. It must be acknowledged that this goal is still far from being achieved and that advances with existing ground-based remote sensing systems will likely be incremental.

References

- Ackerman TP, Stokes GM (2003) The atmospheric radiation measurement program. *Phys Today* 56(1):38–44.
- Bianco L, Cimini D, Marzano FS, Ware R (2005) Combining Microwave radiometer and wind profiler radar measurements for high-resolution atmospheric humidity profiling. *J Atmos Ocean Technol* 22(July):949–965.
- Engelbart D, Monna W, Nash J, Matzler C (eds) (2009). Integrated ground-based remote-sensing stations for atmospheric profiling. EUR 24172 – COST Action 720 final report. COST Office, Brussels.
- Furumoto J, Kurimoto M, Tsuda T (2003). Continuous observations of humidity profiles with the MU radar-RASS combined with GPS and radiosonde measurements. *J Atmos Ocean Technol* 1:23–41.
- Gossard EE, Chadwick RR, Neff WD, Moran KP (1982) The use of ground based Doppler radars to measure gradients, fluxes and structure parameters in elevated layers. *J Appl Meteorol* 21: 211–226.
- Gossard EE, Wolfe DE, Moran KE, Paulus RA, Anderson DK, Rogers LT (1998) Measurements of clear-air gradients and turbulence properties with radar wind profilers. *J Atmos Ocean Technol* 15:321–342.

- Han Y, Westwater ER, Ferrare RA (1997) Applications of Kalman filtering to derive water vapor profiles from Raman lidar and microwave radiometers. *J Atmos Ocean Technol* 14(3):480–487.
- Hogan RJ, O'Connor EJ (2004) Facilitating cloud radar and lidar algorithms: the Cloudnet instrument synergy/target categorization product. Cloudnet Project Documentation.
- Krasnov OA, Russchenberg HWJ (2002) Retrieval of water cloud microphysical parameters from simultaneous RADAR and LIDAR measurements. International Union of Radio Science, XXVII General Assembly, Maastricht, The Netherlands.
- Löhnert U, Crewell S, Simmer C (2004) An integrated approach toward retrieving physically consistent profiles of temperature, humidity, and cloud liquid water. *J Appl Meteorol* 43:1295–1307.
- Mace G, Ackerman TP, Minnis P, Young DF (1998) Cirrus layer microphysical properties derived from surface-based millimeter radar and infrared interferometer data. *J Geophys Res* 103:23207–23216.
- Mace G, Clothiaux EE, Ackerman TP (2001) The composite characteristics of cirrus clouds: bulk properties revealed by one year of continuous cloud radar data. *J Climate* 14:2185–2203.
- Rodgers CD (2000) Inverse methods for atmospheric sounding: theory and practice. World Scientific, Singapore.
- Stankov BB, Westwater ER, Gossard EE (1996) Use of wind profiler estimates of significant moisture gradients to improve humidity profile retrieval. *J Atmos Ocean Technol* 13:1285–1290.
- Stankov BB, Gossard EE, Weber BL, Lataitis RJ, White AB, Wolfe DE, Welsh DC (2003) Humidity gradient profiles from wind profiling radars using the NOAA/ETL advanced signal processing system (SPS). *J Atmos Ocean Technol* 20:3–22.
- Turner DD et al (2004) The QME AERI LBLRTM: a closure experiment for downwelling high spectral resolution infrared radiance 61(22):2657–2675.
- Westwater ER et al (1999) Ground-based remote sensor observations during PROBE in the tropical western Pacific. *Bull Am Meteorol Soc* 80:257–270.